ACS central science

http://pubs.acs.org/journal/acscii

Research Article

Broad Spectrum Antibiotic Xanthocillin X Effectively Kills *Acinetobacter baumannii via* Dysregulation of Heme Biosynthesis

Ines Hübner, Justin A. Shapiro, Jörn Hoßmann, Jonas Drechsel, Stephan M. Hacker, Philip N. Rather, Dietmar H. Pieper, William M. Wuest, and Stephan A. Sieber*

Cite This: *ACS Cent. Sci.* 2021, 7, 488–498

Read Online

ACCESS | Metrics & More | Article Recommendations | Supporting Information

ABSTRACT: Isonitrile natural products exhibit promising antibacterial activities. However, their mechanism of action (MoA) remains largely unknown. Based on the nanomolar potency of xanthocillin X (**Xan**) against diverse difficult-to-treat Gram-negative bacteria, including the critical priority pathogen *Acinetobacter baumannii*, we performed in-depth studies to decipher its MoA. While neither metal binding nor cellular protein targets were detected as relevant for **Xan**'s antibiotic effects, sequencing of resistant strains revealed a conserved mutation in the heme biosynthesis enzyme porphobilinogen synthase (PbgS). This mutation caused impaired enzymatic efficiency indicative of reduced heme production. This discovery led to the validation of an untapped mechanism, by which direct heme sequestration of **Xan** prevents its binding into cognate enzyme pockets resulting in uncontrolled cofactor biosynthesis, accumulation of porphyrins, and corresponding stress with deleterious effects for bacterial viability. Thus, **Xan** represents a promising antibiotic displaying activity even against multidrug resistant strains, while exhibiting low toxicity to human cells.

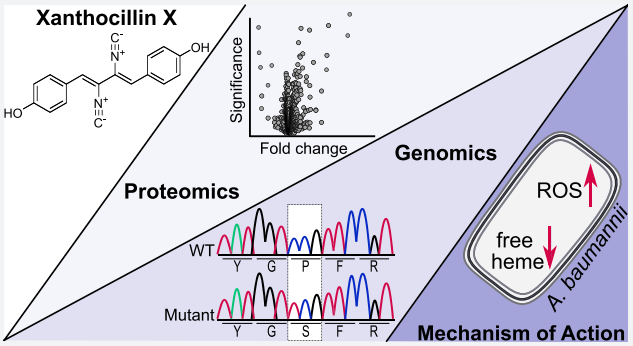

INTRODUCTION

Natural product antibiotics are evolutionarily optimized to hit the soft spots of bacterial viability. Several of these potent drugs have been brought into the clinic in the middle of the 20th century but today suffer from the development of multidrug-resistant bacteria.[1] This situation is exacerbated by a limited scope of cellular targets and adapted bacteria bearing multiple resistance strategies.[2,3] Thus, bioactive compounds with completely new structures and unprecedented mechanisms of action (MoAs) are urgently required. A wealth of diverse natural product scaffolds with antibacterial activity have been identified in the "golden age" of antibiotic discovery. However, their mechanistic and biological characterization is still in its infancy. Thus, the systematic mining of these neglected structures for novel MoAs represents an untapped source of new drugs, going beyond current antibacterial discovery programs mainly focused on synergistic antibiotic combinations or on optimizing existing antibiotic scaffolds.[2,4,5] The situation gets even worse when looking at Gram-negative bacteria, such as *Pseudomonas aeruginosa* and *Acinetobacter baumannii*, which pose a particular threat owing to their dual-membrane envelope that prevents many antibiotics from accessing their targets.[6] Despite considerable effort, no new class of antibiotic has been approved for Gram-negative pathogens in over 50 years.[7,8]

One source of potent antibacterial candidates are isonitrile (also termed isocyanide) natural products which were first discovered by the isolation of xanthocillin X (**Xan**) from *Penicillium notatum* in 1948.[9−11] Thus far, about 200 members of this class have been identified from diverse sources, including fungi (e.g., **Xan**), bacteria (e.g., SF2768), and sponges (e.g., kalihinol A, axisonitrile-3) (Figure 1A), many of them structurally related to **Xan**.[12−16] Isonitrile containing natural products combine unexploited functionality with broad spectrum activity against bacteria, viruses, fungi, and parasites[9,12−19] as well as low human toxicity,[5,18] thus representing an auspicious compound class for drug discovery. For instance, MDN-0057 is known to be active against Gram-negative bacteria such as *A. baumannii*, ranked as a critical pathogen with the highest priority according to the WHO.[5,20] Further, it was shown that secondary and tertiary isocyanides exhibit metabolic stability, making the isonitrile a promising pharmacophore in the discovery and development of novel antimicrobial drugs.[5,21] Despite these features, little is known

Received: December 4, 2020
Published: January 20, 2021

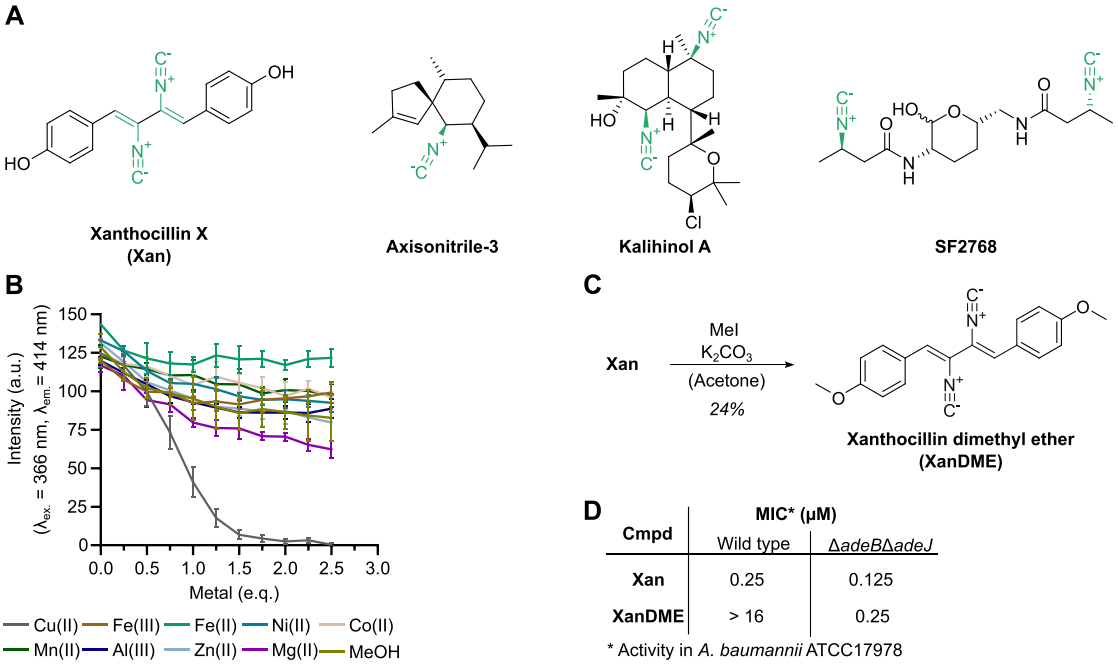

Figure 1. Structures of naturally occurring isonitriles and metal binding ability of **Xan**. (**A**) Structures of natural products **Xan**,[9] axisonitrile-3,[15] kalihinol A, and SF2768.[14,17] (**B**) Fluorescence titration of **Xan** (12.5 μM) with various metals. The data represent average values ± s.d. of independent experiments (n = 3 per group). (**C**) Synthesis of **XanDME** by methylation of **Xan**. (**D**) MICs of **Xan** and **XanDME** in *A. baumannii* ATCC17978 wt and *A. baumannii* ATCC17978 Δ*adeB* Δ*adeJ*,[31] a knockout strain of two efflux pumps (*adeB*, *adeJ*). MICs were determined in n = 3 independent experiments.

about their MoA, which is an indispensable step in drug discovery and lead optimization. So far, binding to transition metals (e.g., Fe, Cu), either directly or complexed in heme, has been associated with isonitrile bioactivity. For example, terpene isonitriles were shown to exert their antiplasmodial activity by binding to heme and thus inhibiting the parasite's vital heme detoxification processes.[22] In addition, the copper chelating ability of SF2768 was linked to antibacterial activity.[23] However, a comprehensive approach for the identification of cellular targets and mechanisms of this compound class is still missing.[24,25]

Here we chose **Xan** as a representative compound for the isonitrile class to decipher its MoA. An initial broad antibacterial screen revealed **Xan** as most active against *A. baumannii*, with a minimum inhibitory concentration (MIC) in the nanomolar range. Unexpectedly, chemical proteomic and genomic studies revealed sequestration of cellular regulatory heme as the main target pathway. Heme binding assays, quantification of regulatory heme, and full proteome analysis point to an unprecedented MoA based on dysregulated heme biosynthesis with catastrophic effects for cell physiology.

RESULTS

Antibacterial Screen. Despite numerous studies on **Xan** biosynthesis,[26,27] a quantitative evaluation of its antibiotic properties against diverse bacterial species, such as clinically relevant pathogens *A. baumannii* and *Klebsiella pneumonia*, is lacking.[9,28] Thus, prior to mechanistic studies we evaluated the antibiotic scope of **Xan** against a panel of Gram-positive and Gram-negative strains. Synthesis of **Xan** commenced according to published procedures and subsequent screening revealed a broad spectrum bioactivity of **Xan** against nearly all strains tested with the notable exception of enterococcal species (Table 1).[29]

Table 1. Activity of Xan against Pathogenic Bacteria[a]

strain	MIC (μM)
Acinetobacter baumannii ATCC19606	0.25−0.5
Acinetobacter baumannii ATCC17978	0.25−0.5
Acinetobacter baumannii AB5075 (MDR)	1
Escherichia coli K12	1
Escherichia coli 536	1
Escherichia coli UTI89	1
Pseudomonas aeruginosa DSM 22644 (PAO1)	3
Klebsiella pneumonia DSM 30104	3
Salmonella typhimurium LT2	3
Salmonella typhimurium TA98	1
Salmonella typhimurium TA100	1
Staphylococcus aureus NCTC 8325 (MSSA)	3
Staphylococcus aureus Mu50 (MRSA)	1
Staphylococcus aureus USA300 (MRSA)	3
Listeria monocytogenes EGD-e	1
Enterococcus faecium DSM 17050 (VRE)	>10
Enterococcus faecalis V583 (VRE)	>10

[a]MICs were determined in n = 3 independent experiments.

Xan killed methicillin-sensitive (MSSA) and methicillin-resistant (MRSA) *Staphylococcus aureus* reference strains as well as Gram-negative pathogens such as *P. aeruginosa, K. pneumonia, Escherichia coli*, and multidrug resistant (MDR) *A. baumannii* AB5075 in the low micromolar range. Strikingly, **Xan** exhibited activity against *A. baumannii* ATCC19606 and ATCC17989 in the nanomolar range. Based on the potent activity against a critical priority pathogen, we selected *A. baumannii* as a surrogate for stepwise in-depth mechanistic studies focusing on metal, protein, and cofactor binding.

Cu^{2+} Binding Is Not the Main Driver of Antibiotic Activity. We commenced our MoA analysis with metal

https://dx.doi.org/10.1021/acscentsci.0c01621
ACS Cent. Sci. 2021, 7, 488−498

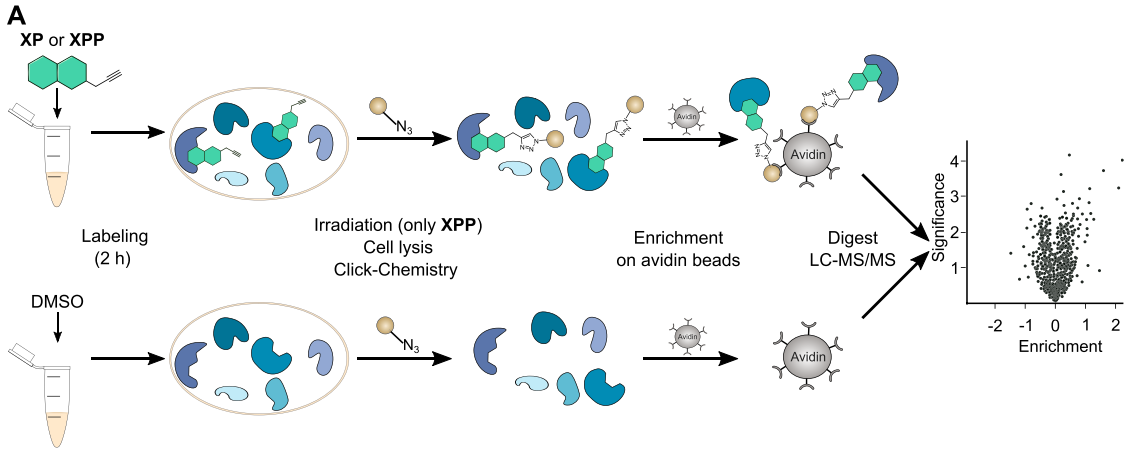

B

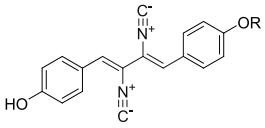

Cmpd	R	MIC* (μM)	MIC** (μM)
Xan	H	1	0.25 - 0.5
XP	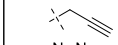	3	3
XPP	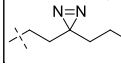	n.d.	3 - 6

*Activity in *E. coli* K12
**Activity in *A. baumannii* ATCC19606

C

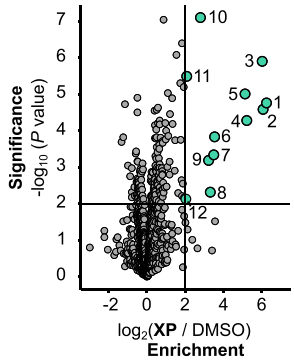

D

#	UniProt ID	Gene	Essentiality
1	P04949	*fliC*	No
2	P39334	*bdcR*	No
3	P0ABK9	*nrfA*	No
4	P37614	*yhhL*	No
5	P76049	*ycjY*	No
6	P55734	*ygaP*	No
7	P77754	*spy*	No
8	P37197	*yhjA*	No
9	P64588	*yqjI*	No
10	P13029	*katG*	No
11	P0AFH8	*osmY*	No
12	P76550	*yffS*	Yes

Figure 2. Target identification by chemical proteomic profiling in *E. coli* and *A. baumannii*. (**A**) Schematic experimental workflow for target identification by ABPP and A*f*BPP. Intact cells were treated with a probe or DMSO (as control), irradiated with UV light (only for **XPP** (A*f*BPP)), lysed, and the labeled proteins clicked to biotin azide. After enrichment on avidin beads, the proteins were enzymatically digested and analyzed by LC-MS/MS measurements. (**B**) Structures of **Xan**, **XP**, and **XPP** with corresponding MICs in *E. coli* K12 and *A. baumannii* ATCC19606. MICs were determined in three independent experiments. The MIC of **XPP** in *E. coli* K12 was not determined (n.d.).(**C**) ABPP experiment using **XP** in *E. coli* K12. The volcano plot shows enrichment of proteins after treatment of *E. coli* cells with **XP** (3 μM) compared with DMSO on a $\log_2$ scale. The vertical and horizontal threshold lines represent a $\log_2$ enrichment ratio of 2 and a $-\log_{10}(P$ value) of 2 (two-sided two-sample *t*-test, $n = 4$ independent experiments per group), respectively. (**D**) Table that allocates proteins above the set threshold from the ABPP experiments. Three essential gene databases for *E. coli* K12 were used to determine essentiality. Protein encoded by gene *yffS* was not outcompeted by **Xan** (Supplementary Figure 3) and was thus not considered as a target of **Xan**.[35−37]

binding assays. Isonitrile SF2768 has been shown to bind copper in bacteria leading to a decrease of the free metal concentration and corresponding disorders in certain copper-dependent enzymatic processes.[23] In order to test if **Xan** exhibits a similar MoA, we performed metal−ligand fluorescence titration using various metals of physiological relevance (Cu(II), Fe(II), Fe(III), Ni(II), Co(II), Mn(II), Al(III), Zn(II), and Mg(II)).[30] In fact, these assays confirmed an exclusive binding of **Xan** to Cu(II) (Figure 1B). In contrast, synthesis and testing of xanthocillin dimethyl ether (**XanDME**, Figure 1C), a naturally occurring derivative, did not reveal a significant interaction with Cu(II), suggesting an important role of the two hydroxy groups for metal binding under our experimental conditions (Supplementary Figure 1). Importantly, while **XanDME** lost its bioactivity (MIC > 16 μM) against *A. baumannii* ATCC17978, its MIC against *A. baumannii* ATCC17978 Δ*adeB*Δ*adeJ*,[31] a knockout strain of two efflux pumps (*adeB*, *adeJ*), was retained with comparable potency to **Xan** (Figure 1D). This suggests that the loss of activity of **XanDME** against wild type (wt) *A. baumannii* is predominantly attributed to a higher efflux rate and that **Xan**'s copper chelating ability is likely not the major contribution to antibacterial activity.

Protein Target Identification by Chemical Proteomics. As the majority of antibiotics target proteins,[3] the second step of our MoA analysis involved chemical proteomics to identify the proteins bound to **Xan** in *A. baumannii* ATCC19606 as well as *E. coli* K12, the best-studied Gram-negative pathogen, as a reference. We thus synthetically equipped **Xan** with either an alkyne tag or with a dual diazirine photo-crosslinker-alkyne tag, required for activity-based protein profiling (ABPP) or affinity-based protein profiling (A*f*BPP), respectively (Figure 2A, Supplementary Figure 2).[32,33] Satisfyingly, the resulting xanthocillin probe (**XP**) and xanthocillin photoprobe (**XPP**) exhibited only a slight increase in MICs of about 3−12-fold compared to **Xan** (Figure 2B). To unravel the identity of the covalently targeted proteins, we performed quantitative gel-free and label-free ABPP analysis.[34] Either intact *E. coli* or *A. baumannii* cells were incubated with 3 μM (MIC concentration) **XP** for 2 h. After cell lysis, labeled proteins were clicked to biotin azide, enriched on avidin beads, and analyzed *via* mass spectrometric (liquid chromatography−tandem mass spectrometry (LC-MS/MS)) analysis. To exclude unspecific avidin binding, we included a dimethyl sulfoxide (DMSO) control. In order to confirm that **XP** and **Xan** address the same binding sites, we performed

https://dx.doi.org/10.1021/acscentsci.0c01621
ACS Cent. Sci. 2021, 7, 488−498

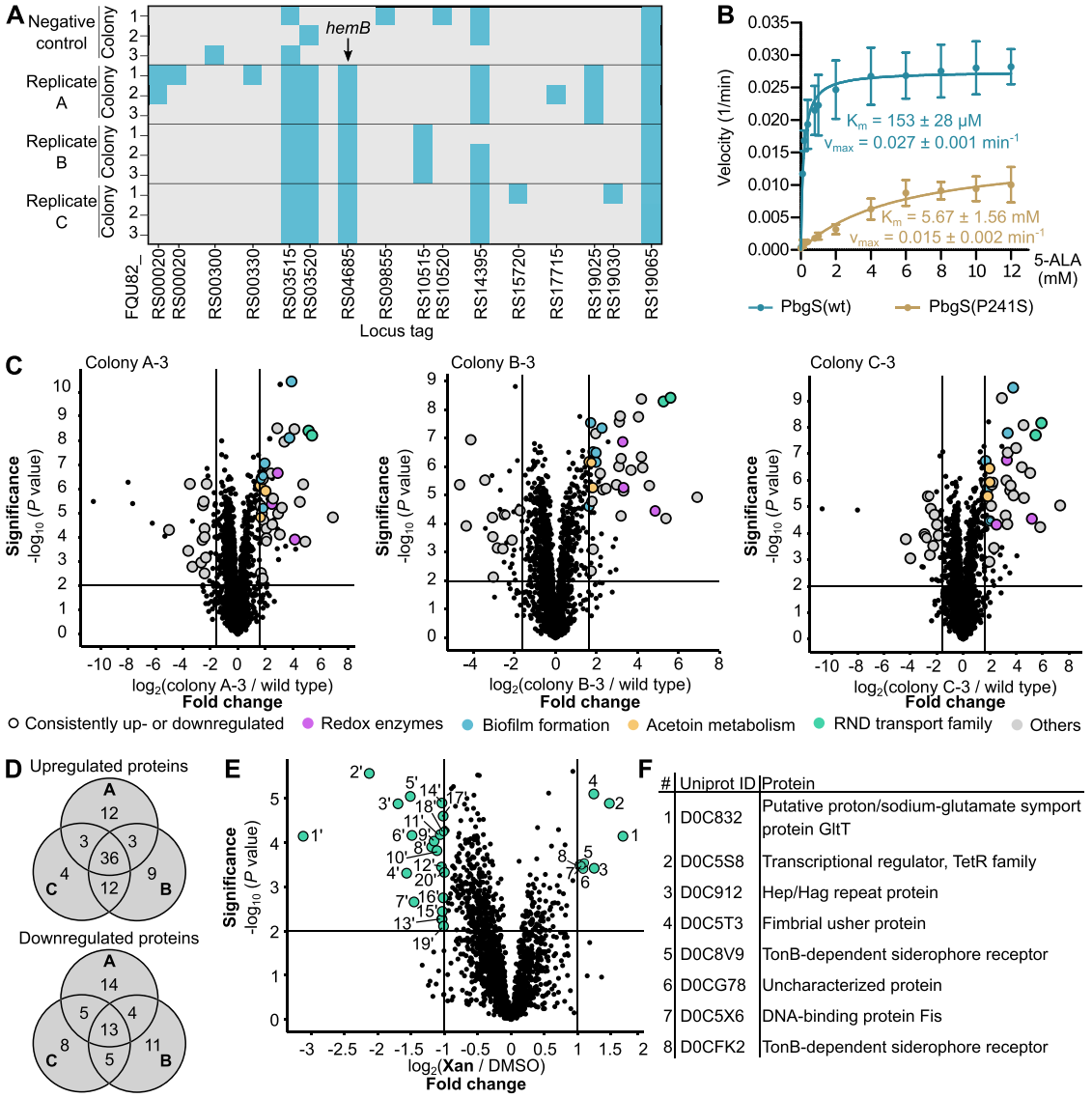

Figure 3. Analysis of **Xan**-resistant mutants and full proteome analysis of **Xan**-treated *A. baumannii*. (**A**) Sequence analysis of **Xan**-resistant isolates. Three colonies from each independent experiment were sequenced and compared to three colonies of the negative control. Mutations are ordered according to the recently published genome sequence of *A. baumannii* ATCC19606 (CP045110, chromosome, and CP45108 plasmid p1ATCC19606). Space between locus tags was omitted, if adjacent genes were mutated. (**B**) Activity assay of PbgS(wt) and PbgS(P241S). All data represent mean values ± s.d. of averaged duplicates of independent experiments (n = 3 per group). (**C**) Full proteome analysis of **Xan**-resistant colonies compared to *A. baumannii* wt. The volcano plots show the change of protein levels on a $\log_2$ scale. The vertical and horizontal threshold lines represent a $\log_2$ change of 1.6 and −1.6 and a $-\log_{10}(P$ value) of 2 (two-sided two-sample t-test, n = 4 independent experiments per group), respectively. Black circle represents proteins up- or downregulated consistently in all three colonies. Violet, blue, and orange dots represent proteins involved in protection against oxidative stress, biofilm formation, and acetoin metabolism, respectively.[44−47] Green and gray dots represent proteins that belong to the resistance-nodulation-division (RND) transporter family and other categories, respectively.[48] (**D**) Venn-diagrams showing consistently up- and downregulated proteins in all three colonies that are above the set thresholds of full proteome analysis (C). (**E**) Full proteome analysis of **Xan**-treated *A. baumannii* wt. The vertical and horizontal lines represent a $\log_2$ change of 1 and −1 and a $-\log_{10}(P$ value) of 2 (two-sided two-sample t-test, n = 4 independent experiments per group), respectively. (**F**) Table that allocates proteins above the set threshold of full proteome analysis (E).

competitive labeling, in which we pretreated either *E. coli* or *A. baumannii* cells with excess of **Xan** (30 µM) before **XP** was added. Enrichment of several proteins by **XP** in both strains indicated substantial covalent binding (Figure 2C, Supplementary Figure 4A). Additionally, competitive labeling led to a significant decrease of enriched proteins (Supplementary Figures 3A and 4B). Proteins were further considered as targets only if they were enriched by **XP** and outcompeted by **Xan**. All proteins that fulfilled these criteria in *A. baumannii* and *E. coli* exhibit nonessential cellular functions (Figures 2D, Supplementary Figure 3B, and 4C).[35−38] Comparison between hits of both strains revealed catalase-peroxidase (CAT, *katG*) as the only overlapping target protein, which we cloned and overexpressed for a closer inspection. While gel-based labeling of recombinantly expressed and purified *A. baumannii* CAT (*Ab*CAT; UniProt ID: D0CAQ1) and *E. coli* CAT (*Ec*CAT; UniProt ID: P13029) validated a covalent binding mode (Supplementary Figure 5), no impact of **Xan** on the enzyme activity was observed, excluding it as a relevant molecular target (Supplementary Figure 6). As noncovalent targets could

https://dx.doi.org/10.1021/acscentsci.0c01621
ACS Cent. Sci. 2021, 7, 488−498

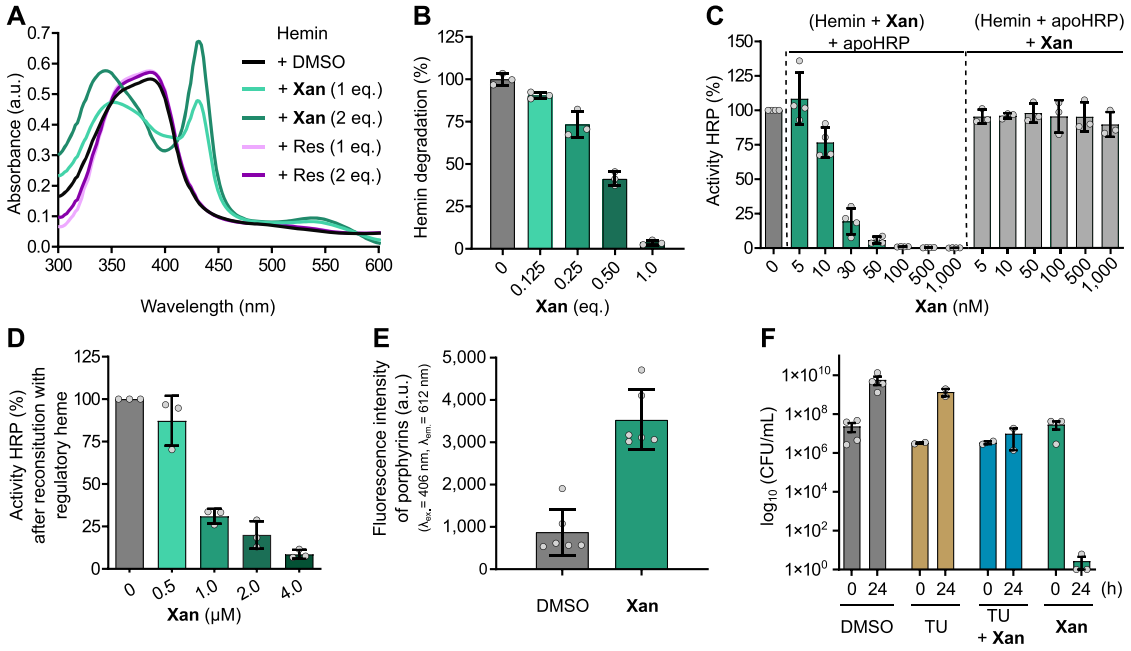

Figure 4. Validation of **Xan**'s binding to heme and the cellular consequences. (**A**) UV−vis spectra of hemin (20 μM) with DMSO (black), **Xan** (20 μM, light green and 40 μM, dark green), resveratrol (Res) (20 μM, light violet and 40 μM, dark violet) in 200 mM HEPES (pH 7.0). Data represent averaged technical duplicates, and the figure is representative of n = 3 independent experiments. Supplementary Figure 12A contains the structure of Res. (**B**) Inhibition of the GSH-mediated destruction of hemin by **Xan**. Values represent mean ± s.d. of averaged triplicates of independent experiments (n = 3) and normalized to the DMSO-treated control. (**C**) *In vitro* activity assay of reconstituted holoHRP in the presence of various concentrations of **Xan**. Hemin (5 nM) was preincubated with either **Xan** (green bars) or apoHRP (light gray bars, 5 μM) followed by addition of apoHRP or **Xan**, respectively, and activity of holoHRP was subsequently measured. Averaged technical duplicates were normalized to the respective DMSO-treated samples and values represent mean ± s.d. of independent experiments (n = 3). (**D**) Reconstitution activity assay of holoHRP in *A. baumannii* cell lysate after treatment of intact cells with various concentrations of **Xan** for 30 min. ApoHRP (final concentration 10 μM) was added to cell lysates and activity of holoHRP was measured. Averaged technical quadruplicates were normalized to the respective DMSO-treated samples and values represent mean ± s.d. of independent experiments (n = 3). Noteworthy, at low concentrations of **Xan** a higher activity, both *in vitro* and in intact *A. baumannii*, was observed for unknown reasons (Supplementary Figure 12F and G). (**E**) Detection of accumulated porphyrins by fluorescence spectroscopy. Intact *A. baumannii* ATCC19606 were incubated with **Xan** (1 μM) for 1 h. After cell lysis, porphyrins were extracted, and fluorescence spectra were recorded (λ_{ex} = 406 nm, Supplementary Figure 13A). Data represent mean values ± s.d. of fluorescence intensities (λ_{ex} = 406 nm, λ_{em} = 612 nm) of independent experiments (n = 6). (**F**) Protective effect of thiourea (TU) on **Xan**-treated *A. baumannii* ATCC19606. DMSO (gray bars), TU (150 mM, yellow bars), **Xan** (4 μM, green bars), TU (150 mM), and **Xan** (4 μM, blue bars) were added to *A. baumannii* ATCC19606 and cells were incubated for 24 h. After 0 and 24 h viable cells (CFU/mL) were determined in quadruplicates. Data represent mean values ± s.e.m of n = 4 (DMSO), n = 3 (**Xan**), and n = 2 (TU, TU and **Xan**) independent experiments.

be involved in **Xan**'s MoA, we performed *Af*BPP in *A. baumannii*. Intact cells were incubated with 3 μM of **XPP**, irradiated with ultraviolet light to form a covalent linkage with the putative target protein, lysed, clicked to biotin azide, enriched and analyzed *via* LC-MS/MS. Again, no essential proteins were among the enriched hits (Supplementary Figures 7 and 8) suggesting a largely proteome-independent MoA.

Xan-Resistant *A. baumannii* Mutants Reduce Heme Levels. With a lack of evidence for metals or proteins being involved in **Xan**'s MoA, we sought to generate resistant mutants for sequencing of altered cellular targets, a common approach to investigate an antibiotic MoA.[24] While attempts to generate resistant colonies by spontaneous mutation on agar plates failed, repeated passaging of *A. baumannii* in the presence of different compound concentrations (0.25−4× MIC) was successful after 11 days. Although **Xan** exhibited a drop in antibacterial activity after a few passages, the resistance development of the control antibiotic ciprofloxacin was significantly faster (Supplementary Table 1). The slower resistance formation compared to standard antibiotics is in accordance with a previous study that treated staphylococci with sub-MICs of **Xan** for 240 days, which failed to produce any resistant strains.[9] Whole-genome sequencing of three mutants each from three independent experiments and three colonies of the negative control unveiled that only the gene *hemB* encoding the enzyme porphobilinogen synthase (PbgS) was consistently mutated in response to **Xan** but not upon DMSO treatment (Figure 3A). Intriguingly, a single missense mutation within *hemB*, leading to amino acid change P241S, was constantly found in all nine resistant colonies. PbgS is an essential enzyme in *A. baumannii* that catalyzes the first common step in the biosynthesis of all tetrapyrroles.[38,39] Sequence alignment clearly illustrated the mutation being close to the active site (Supplementary Figure 9).

To evaluate the impact of this mutation on the enzyme activity, we cloned PbgS(wt) and PbgS(P241S) into expression vectors. All attempts to purify the recombinant proteins failed due to aggregation (Supplementary Discussion 1, Supplementary Figure 10). Satisfyingly, direct transformation of *A. baumannii* ATCC19606 with tag free plasmids pVRL2-*abhemB*$_{wt}$ and pVRL2-*abhemB*$_{P241S}$ resulted in soluble proteins and active PbgS(wt) upon arabinose induction.[40] Additionally, label-free LC-MS/MS analysis revealed a comparable amount of overexpressed wt and mutant protein in cell lysates (Supplementary Figure 11B), which wereused for the activity assays. In order to subtract the basal activity of the native

https://dx.doi.org/10.1021/acscentsci.0c01621
ACS Cent. Sci. 2021, 7, 488−498

PbgS(wt), *A. baumannii* wt lysate was included as control. Determination of the Michaelis−Menten constant K_m of 153 μM for PbgS(wt) toward the substrate 5-aminolevulinic acid (5-ALA) was in line with literature data of homologous proteins.[41−43] Importantly, PbgS(P241S) was still active albeit with a 37-fold increase in K_m (5670 μM) indicating that the mutation resulted in a significant drop in affinity for 5-ALA (Figure 3B) and consequently in enzyme efficiency (see Supplementary Discussion 2). In order to investigate if PbgS is a direct target of **Xan**, we preincubated the wt enzyme with the compound and determined the residual activity. No inhibitory effect was observed under the tested conditions, corroborating our chemical proteomic data, in which this protein was also not significantly enriched (Supplementary Figure 11A). Thus, the consistent mutation of this essential heme biosynthesis enzyme throughout all resistant mutants conceivably affects the tetrapyrrole biosynthesis rather than directly influencing target binding of **Xan**. To examine these consequences in more detail on the cellular level, we compared the mutant strains to *A. baumannii* wt in a full proteome analysis. *A. baumannii* wt and three mutants (A-3, B-3, and C-3) were grown in the absence of **Xan** until reaching the mid-exponential phase (OD_{600} of 2.0) and subsequently harvested for label-free LC-MS/MS analysis (Figure 3C). All three mutants showed a high overlap of upregulated proteins (Figure 3D). Among those, proteins involved in protection against oxidative stress (catalase, two heme-oxygenase like proteins[44]), biofilm formation (e.g., protein CsuC/E, spore coat protein U domain protein[45,46]), acetoin metabolism (e.g., TPP-dependent acetoin dehydrogenase complex[47]) and efflux transporters (RND transporter, efflux transporter (RND family)[48]) were upregulated (Supplementary Table 2 and 3). The upregulation of two heme oxygenase-like proteins in all mutants was noteworthy as these enzymes catalyze the degradation of heme. In combination with an impaired porphobilinogen synthesis *via* mutated PbgS, their increased expression is suggestive of a need to reduce heme levels during resistance formation to **Xan**. Reduced heme levels are known to limit electron flow in the electron transport chain and thus might shift metabolism from respiration to fermentation.[49] *A. baumannii* is considered to be a strict aerobe; however, a recent paper showed first evidence of the survival of *A. baumannii* under anaerobic conditions.[50] This is in agreement with the upregulation of enzymes metabolizing acetoin, a major fermentation product in bacteria.[51] In a complementary experiment, we investigated the direct effects of **Xan** on heme biosynthesis by comparing the full proteomes of treated and untreated *A. baumannii*. Cells were grown in the presence of either 125 nM **Xan** (0.5× MIC) or DMSO and harvested in mid-exponential phase (OD_{600} of 2.0). Interestingly, a putative proton/sodium glutamate symport protein showed highest upregulation (>3-fold) *via* LC-MS/MS analysis (Figure 3E and F, Supplementary Table 4).[52] In bacteria, glutamate is needed to generate 5-ALA, a precursor of heme. Upregulation of this symporter hints at an increased demand for glutamate and thus at an enhanced heme biosynthesis in the presence of **Xan**. Furthermore, increased expression of two TonB-dependent siderophore receptors, transporting ferric chelates, suggests an elevated demand for iron uptake, the substrate for the last step of the heme biosynthesis.[53] Taken together, the full proteome analysis of **Xan**-resistant and **Xan**-treated *A. baumannii* points toward elevated heme production under antibiotic treatment and a consequent attenuation of heme biosynthesis as a resistance strategy.

Xan Binds to Heme *in Vitro*. The observed effect of **Xan** on heme biosynthesis, independent of protein binding, can be consolidated *via* a direct interaction of isonitriles with the heme cofactor. Despite a lack of comprehensive data, a previous report showed that the binding of different isonitrile compounds affected the spectral characteristics of oxidized heme (hemin), which was further linked to antimalarial activity.[22] Elucidating this hypothesis in more detail, we examined the effect of **Xan** on the visible absorption spectrum of hemin. In aqueous buffer (pH 7), hemin exhibits a Soret absorption band with a peak at 390 nm. After addition of **Xan**, the Soret band is red-shifted to 438 nm and a peak at 550 nm appears in a concentration dependent manner (Figure 4A). This alteration of the absorbance spectrum highlights a direct interaction of hemin with **Xan**. As a control we included resveratrol (Res), a molecule structurally highly similar to **Xan** but without isonitrile groups (Supplementary Figure 12A). The lack of binding emphasizes the relevance of isonitriles for productive interactions with hemin. **XP** and **XanDME** show similar alteration of the absorbance spectrum of hemin, indicating that the hydroxyl groups are not involved in the interaction with hemin (Supplementary Figure 12C and D). In order to investigate whether **Xan** binds to iron in hemin a UV−vis spectrum of protoporphyrin IX (PPIX), iron-free hemin, with and without the addition of **Xan** was recorded. Since no change in the spectrum was observed after addition of **Xan**, an interaction between **Xan** and iron can be assumed (Supplementary Figure 12B). Interestingly, complexation by **Xan** or **XanDME** effectively prevented glutathione (GSH)-mediated hemin degradation in a dose dependent response and even equimolar amounts of these compounds were sufficient to fully block hemin degradation (Figure 4B, Supplementary Figure 12E).[22,54]

Xan Reduces Effective Regulatory Heme Level. In cells, heme serves as the prosthetic moiety of many hemoproteins that are involved in essential biological functions including oxygen binding and metabolism (e.g., hemoglobin and oxidases) and electron transfer (e.g., cytochromes).[55] In addition, heme acts as a regulator for specific proteins (heme-responsive proteins) by binding in an on/off mechanism to the heme regulatory motif. It is believed that heme-responsive proteins are regulated by free heme, heme from low affinity heme-binding proteins, or newly synthesized heme, which we will collectively refer to as regulatory heme (RH).[56] Given the coordination of **Xan** to heme, it is conceivable, that **Xan** may unbalance heme's fine-tuned regulatory role in cells and reduces levels of RH. To inspect RH levels, we applied a colorimetric assay based on horse radish peroxidase (HRP) in its cofactor free form (apoHRP), which after reconstitution with RH becomes active holoHRP.[56] The utility of this assay was tested *via* preincubation of hemin with increasing concentrations of **Xan** in PBS prior to the addition of apoHRP (5 μM). Decreasing HRP activity with increasing concentration of **Xan** clearly showed that **Xan**'s binding to hemin prevents reconstitution of holoHRP (Figure 4C, green bars). A direct inhibition of holoHRP by **Xan** was excluded *via* preincubation of apoHRP with hemin prior to addition of **Xan**. No drop in activity even at high concentrations of **Xan** was observed (Figure 4C, gray bars). Next, we applied the HRP assay to intact *A. baumannii* cells and measured intracellular RH after treatment with either **Xan** or DMSO

https://dx.doi.org/10.1021/acscentsci.0c01621
ACS Cent. Sci. 2021, 7, 488−498

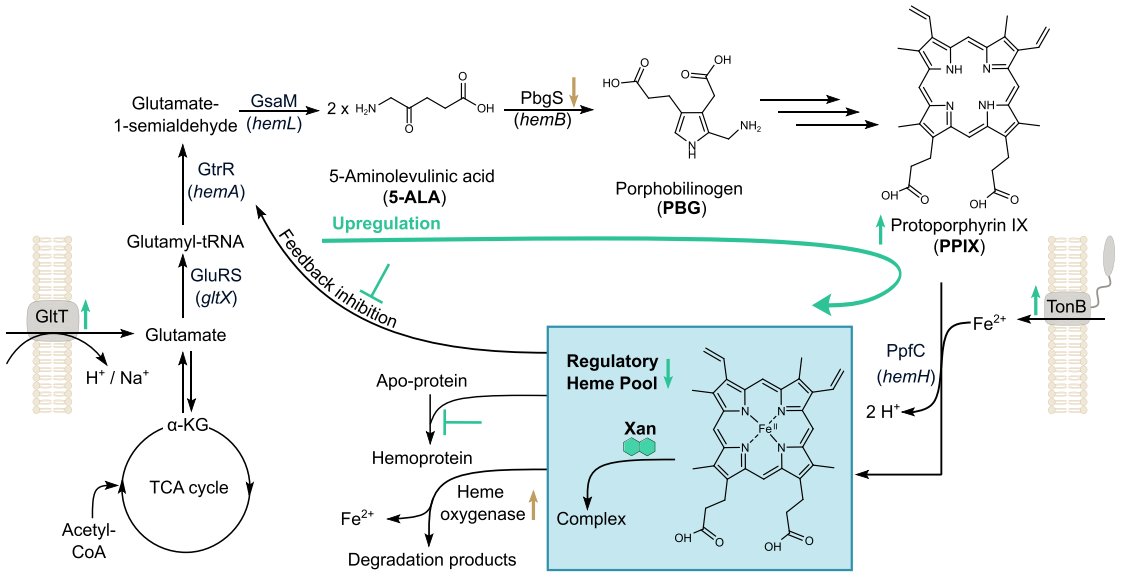

Figure 5. Dysregulation of heme biosynthesis by **Xan**. Hypothesis of **Xan**'s MoA is based on experimental evidence within this study. Full proteome analysis of **Xan**-treated *A. baumannii* revealed a putative proton/sodium-glutamate symport protein GltT as well as two TonB-dependent siderophore receptors as significantly upregulated proteins pointing to enhanced demand for heme biosynthesis substrates, glutamate and iron. Extraction of porphyrins of **Xan**-treated *A. baumannii* validated the accumulation of tetrapyrroles. UV−vis spectrum showed an interaction between hemin and **Xan**. Further, reconstitution assay using apoHRP let us conclude that complex formation of **Xan** with hemin leads to a reduced effective level of RH and thus to an impaired regulatory role of heme. Conceivable consequences are the inability of hemoproteins to acquire heme for their normal metabolic function or uncontrolled biosynthesis by hampered feedback inhibition. In-depth analysis of **Xan**-resistant isolates showed a shared amino acid mutation P241S in PbgS that leads to a significant drop in enzyme efficiency and thus counteracts the upregulation by **Xan**. Further, **Xan**-resistant colonies upregulate heme degrading enzymes (heme oxygenases) as well as proteins involved in biofilm formation, RND transporters, and acetoin metabolism. Abbreviations include the following: TCA, tricarboxylic acid cycle; α-KG, α-ketoglutarate; GluRS (*gltX*), glutamyl-tRNA synthetase; GtrR (*hemA*), glutamyl-tRNA reductase; GsaM (*hemL*), glutamate-1-semialdehyde-2,1-aminomutase; PbgS (*hemB*), porphobilinogen synthase; PpfC (*hemH*), protoporphyrin IX ferrochelatase. Cellular effects induced by **Xan** treatment are shown by green arrows, while effects of resistance formation are indicated by brown arrows.

for 30 min. Upon cell lysis, we detected a clear decrease of RH levels with increasing concentration of **Xan** (Figure 4D). These results show that **Xan** effectively sequesters heme and thereby limits the ability of hemoproteins to acquire this crucial cofactor. As a consequence, their physiological metabolic function is impaired, as shown for HRP.

In addition, heme controls its own synthesis *via* binding to glutamyl-tRNA reductase (GtrR) by an allosteric feedback mechanism.[57] This feedback control, which may also be impaired, is essential to the viability of cells as excess of heme is highly toxic to cells.

Reduced Regulatory Heme Level Leads to Accumulation of Porphyrins. Uncontrolled heme biosynthesis induced by impaired feedback inhibition would lead to enhanced tetrapyrrole levels. To validate this hypothesis, we fluorescently quantified porphyrin intermediates using an established protocol.[58−60] *A. baumannii* was incubated with either **Xan** or DMSO for 1 h, porphyrins were extracted from cell lysate and fluorescence spectra subsequently measured (λ_{ex} = 406 nm) (Supplementary Figure 13A). In accordance with enhanced heme biosynthesis, the fluorescence signal of **Xan**-treated *A. baumannii* was significantly increased (Figure 4E) demonstrating accumulation of fluorescent porphyrins. Intriguingly, incubation of *A. baumannii* with **Xan** for an elongated time of 4 h led to a brown-red colored pellet, highlighting the dramatic extent of dysregulated porphyrin production (Supplementary Figure 13B). Accumulation of porphyrins is known to generate reactive oxygen species (ROS) with deleterious effects on bacterial viability.[61] Thus, the biological effect of elevated porphyrin levels was investigated *via* time-kill experiments to explore if the addition of a ROS scavenger is able to counterbalance **Xan**'s antibiotic activity.[62] *A. baumannii* treatment with 4 μM **Xan** eliminated all bacteria within 24 h (Figure 4F). Interestingly, addition of thiourea (TU) overrode the bactericidal effect of **Xan**, indicating that cell death is induced by ROS, which in turn is presumably caused by porphyrin accumulation.

Xan Shows a Synergistic Effect with Gentamicin. Synergistic combination of two antimicrobial agents is generally an effective strategy to fight resistance.[4] The activity of aminoglycoside antibiotics, e.g., gentamicin (Gen), has previously been shown to be influenced by altered heme biosynthesis.[49,63,64] Thus, we determined fractional inhibitory concentrations (FICs) in *A. baumannii* ATCC19606 (Gen-sensitive) and *A. baumannii* AB5075 (Gen-resistant[65]) using checkerboard assays. In fact, **Xan** potentiated the activity of Gen against both strains with FIC indices in the range of 0.3125−0.375 (Supplementary Table 5). This means that, in Gen-resistant *A. baumannii* AB5075, 0.25× MIC of **Xan** increased the susceptibility of Gen from 800 to 50−100 μM. In line with published data, **Xan** did not show any significant toxicity in human cells up to its solubility limit of 10 μM highlighting a suitable therapeutic window for single or combination treatment (Supplementary Figure 14).[9,18,28]

DISCUSSION

The current antibiotic crisis demands unconventional solutions including a renewed consideration of potential antibiotic targets and alternate therapeutic strategies, for which new pharmacophore structures are desperately needed.[7,8] One

https://dx.doi.org/10.1021/acscentsci.0c01621
ACS Cent. Sci. 2021, 7, 488−498

source of potent antibacterial candidates are natural products, such as isonitriles, that combine unique functionality with bioactivity. As little was known about the MoA of isonitriles, we chose **Xan** as a representative compound. Based on the intriguing activity of **Xan** against several Gram-negative pathogens, we initiated a multidisciplinary target analysis in *A. baumannii* to unravel its MoA. Recently, copper complexation was postulated as a major mechanism of isonitrile compounds. However, while we confirmed selective binding of Cu(II) to **Xan**, this complexation is likely not the major contribution to antibacterial activity. In addition, as ABPP and *Af*BPP studies only revealed target proteins with nonessential cellular functions, we concluded an unconventional MoA beyond the major scope of current antibiotics. Generation of **Xan**-resistant mutants finally provided a breakthrough by identification of PbgS as the only commonly mutated enzyme among all strains, bearing a P241S modification close to the active site. Activity assays revealed that the mutated PbgS exhibits a significantly lower efficiency (k_{cat}/K_m) for substrate 5-ALA, suggesting a reduced rate of tetrapyrrole synthesis. Since inhibition assay excluded PbgS as a direct target of **Xan**, whole proteome analysis of **Xan**-resistant mutants versus wt, as well as **Xan**-treated versus DMSO-treated wt *A. baumannii*, were performed. Upregulation of a putative proton/sodium glutamate symport protein as well as TonB-dependent siderophore receptors in **Xan**-treated wt bacteria suggests an enhanced heme biosynthesis, as demonstrated by elevated cellular porphyrin levels. By contrast, mutant bacteria showed upregulation of two heme degrading enzymes and acetoin metabolizing enzymes, suggesting a reduced porphyrin level and a switch to fermentation. Finally, direct sequestration of heme by **Xan** results in an inability of heme-dependent enzymes to access RH and corresponding reduced RH levels.

How does **Xan** stimulate heme biosynthesis and kill bacteria? Taken together, our results consolidate in a MoA, by which **Xan** enters bacterial cells and binds to free regulatory heme (Figure 5). This complexation impairs binding of RH to essential hemoproteins (as shown in the HRP assay) and disrupts its regulatory role, including the control of its own biosynthesis by negative feedback inhibition.[57] As a consequence, uncontrolled heme biosynthesis leads to elevated porphyrin levels (spectroscopic analysis) which demands enhanced uptake of precursors (upregulation of glutamate symporter and TonB-dependent siderophore receptors). Negative effects of this dysregulation for viability are manifold. On one hand, essential hemoproteins such as enzymes involved in the electron transport chain (e.g., succinate dehydrogenase cytochrome b_{556} subunit, cytochrome bo_3 ubiquinol oxidase subunit)[66] cannot carry out their biological function due to the lack of their functional cofactor. On the other hand, elevated porphyrin levels induce deleterious ROS (scavenger assay). Another conceivable consequence is that the higher demand for glutamate, caused by the upregulated heme biosynthesis, leads to a glutamate deficiency within bacteria. As a result, bacteria counteract this pressure by a single mutation in a regulatory enzyme of heme biosynthesis, PbgS, catalyzing the formation of porphobilinogen from 5-ALA. This mutation causes a significant slow-down of the production rate which, together with the expression of heme-degrading enzymes, is sufficient to balance the effects of **Xan** on RH. As these levels might be insufficient to supply the electron chain with cofactors, the cell switches to fermentative metabolism, as indicated by the upregulation of acetoin metabolizing enzymes.

Of note, while **Xan** exhibited broad spectrum activity against a panel of bacteria that rely on heme biosynthesis, two strains, *Enterococcus faecalis* and *Enterococcus faecium*, were insensitive to treatment. Interestingly, both strains represent natural heme auxotrophs which rely on heme uptake rather than endogenous biosynthesis.[67]

Xan exhibits remarkable activity against Gram-negative bacteria, a rare trait given the high permeability barrier of these organisms. While more studies on the mechanism of **Xan** uptake are needed in future experiments, we already showed that methylation of the free alcohols of **Xan** abolished antibiotic activity by efflux. Thus, unique structural features, potent broad-spectrum antibacterial activity, limited toxicity,[9,18,28] and an unprecedented MoA highlight **Xan** as a promising starting point for further development and emphasize the potential of yet unexplored isonitriles.[13,68]

■ ASSOCIATED CONTENT

Supporting Information

The Supporting Information is available free of charge at https://pubs.acs.org/doi/10.1021/acscentsci.0c01621.

Supplementary Discussion, Tables, and Figures as well as applied methods and ^{1}H and ^{13}C NMR spectra (PDF)

Target identification related proteomic data (XLSX)

Overview of mutations (XLSX)

Full proteome analysis related proteomic data (XLSX)

Genome assembly (PDF)

■ AUTHOR INFORMATION

Corresponding Author

Stephan A. Sieber − *Center for Functional Protein Assemblies at the Department of Chemistry and Chair of Organic Chemistry II, Technische Universität München, Garching D-85748, Germany;* orcid.org/0000-0002-9400-906X; Email: stephan.sieber@tum.de

Authors

Ines Hübner − *Center for Functional Protein Assemblies at the Department of Chemistry and Chair of Organic Chemistry II, Technische Universität München, Garching D-85748, Germany;* orcid.org/0000-0002-3002-2978

Justin A. Shapiro − *Department of Chemistry, Emory University, Atlanta, Georgia 30322, United States;* orcid.org/0000-0001-9891-0464

Jörn Hoßmann − *Microbial Interactions and Processes Research Group, Helmholtz Centre for Infection Research, Braunschweig 38124, Germany*

Jonas Drechsel − *Center for Functional Protein Assemblies at the Department of Chemistry and Chair of Organic Chemistry II, Technische Universität München, Garching D-85748, Germany;* orcid.org/0000-0002-2891-263X

Stephan M. Hacker − *Department of Chemistry, Technische Universität München, Garching D-85748, Germany;* orcid.org/0000-0001-5420-4824

Philip N. Rather − *Emory Antibiotic Resistance Center and Department of Microbiology and Immunology, Emory University School of Medicine, Atlanta, Georgia 30322, United States; Research Service, Atlanta VA Medical Center, Decatur, Georgia 30033, United States*

https://dx.doi.org/10.1021/acscentsci.0c01621
ACS Cent. Sci. 2021, 7, 488−498

Dietmar H. Pieper − *Microbial Interactions and Processes Research Group, Helmholtz Centre for Infection Research, Braunschweig 38124, Germany*

William M. Wuest − *Department of Chemistry, Emory University, Atlanta, Georgia 30322, United States; Emory Antibiotic Resistance Center, Emory University School of Medicine, Atlanta, Georgia 30322, United States;* orcid.org/0000-0002-5198-7744

Complete contact information is available at: https://pubs.acs.org/10.1021/acscentsci.0c01621

Author Contributions

I.H. and S.A.S. designed the experiments and wrote the manuscript with input from all the authors. W.M.W. helped to interpret the results. I.H. conducted the synthesis of all compounds, antimicrobial screening, cloning of proteins, gel- and MS-based labeling, whole proteome analysis, activity assays, all heme related assays, porphyrin quantification, scavenging assay, checkerboard assay, and MTT assay. J.A.S. and W.M.W. performed the metal binding assay. J.H. and D.H.P. conducted the whole-genome sequencing of resistant bacterial isolates and analyzed the related data. J.D. and I.H. carried out MS data analysis. S.M.H. helped with whole proteome analysis and contributed proteomics expertise. P.N.R. helped with antimicrobial screening in *A. baumannii* wt and mutant strains.

Funding

I.H. was supported by a doctoral fellowship of the Studienstiftung des Deutschen Volkes. S.M.H. acknowledges financial support by a Liebig fellowship of the Fonds der Chemischen Industrie. J.A.S. was supported by a postdoctoral fellowship from the National Institutes of Health (GM133091). W.M.W. acknowledges financial support from the National Institute of General Medical Sciences (GM119426) and the Georgia Research Alliance based in Atlanta, GA. P.N.R. is supported by funding from the U.S. Department of Veterans Affairs I01 BX001725 and IK6BX004470 and NIH awards R21AI142489 and R01AI072219.

Notes

The authors declare no competing financial interest.

The mass spectrometry proteomics data have been deposited at the ProteomeXchange Consortium *via* the PRIDE[69] partner repository with the data set identifier PXD021400. Whole-genome sequencing data and metadata are available on the SRA repository under the Bioproject number PRJNA639720.

■ ACKNOWLEDGMENTS

We thank M. Wolff and K. Bäuml for excellent technical support and Dr. L. Borges and Dr. H. Junca for their kind help with writing the method section "Whole-Genome Sequencing" and the submission of the data on the SRA repository. We thank Prof. P. Visca for providing us with the plasmid pVRL2.

■ REFERENCES

(1) Cassini, A.; Högberg, L. D.; Plachouras, D.; Quattrocchi, A.; Hoxha, A.; Simonsen, G. S.; Colomb-Cotinat, M.; Kretzschmar, M. E.; Devleesschauwer, B.; Cecchini, M.; Ouakrim, D. A.; Oliveira, T. C.; Struelens, M. J.; Suetens, C.; Monnet, D. L.; Strauss, R.; Mertens, K.; Struyf, T.; Catry, B.; Latour, K.; Ivanov, I. N.; Dobreva, E. G.; Tambic Andraševic, A.; Soprek, S.; Budimir, A.; Paphitou, N.; Žemlicková, H.; Schytte Olsen, S.; Wolff Sönksen, U.; Märtin, P.; Ivanova, M.; Lyytikäinen, O.; Jalava, J.; Coignard, B.; Eckmanns, T.; Abu Sin, M.; Haller, S.; Daikos, G. L.; Gikas, A.; Tsiodras, S.; Kontopidou, F.; Tóth, Á.; Hajdu, Á.; Guólaugsson, Ó.; Kristinsson, K. G.; Murchan, S.; Burns, K.; Pezzotti, P.; Gagliotti, C.; Dumpis, U.; Liuimiene, A.; Perrin, M.; Borg, M. A.; de Greeff, S. C.; Monen, J. C.; Koek, M. B.; Elstrøm, P.; Zabicka, D.; Deptula, A.; Hryniewicz, W.; Caniça, M.; Nogueira, P. J.; Fernandes, P. A.; Manageiro, V.; Popescu, G. A.; Serban, R. I.; Schréterová, E.; Litvová, S.; Štefkovicová, M.; Kolman, J.; Klavs, I.; Korošec, A.; Aracil, B.; Asensio, A.; Pérez-Vázquez, M.; Billström, H.; Larsson, S.; Reilly, J. S.; Johnson, A.; Hopkins, S. Attributable Deaths and Disability-Adjusted Life-Years Caused by Infections with Antibiotic-Resistant Bacteria in the EU and the European Economic Area in 2015: A Population-Level Modelling Analysis. *Lancet Infect. Dis.* **2019**, *19* (1), 56−66.

(2) Walsh, C. T.; Wencewicz, T. A. Prospects for New Antibiotics: A Molecule-Centered Perspective. *J. Antibiot.* **2014**, *67* (1), 7−22.

(3) Kohanski, M. A.; Dwyer, D. J.; Collins, J. J. How Antibiotics Kill Bacteria: From Targets to Networks. *Nat. Rev. Microbiol.* **2010**, *8* (6), 423−435.

(4) Xu, X.; Xu, L.; Yuan, G.; Wang, Y.; Qu, Y.; Zhou, M. Synergistic Combination of Two Antimicrobial Agents Closing Each Other's Mutant Selection Windows to Prevent Antimicrobial Resistance. *Sci. Rep.* **2018**, *8* (1), 1−7.

(5) Brown, D. G.; Lister, T.; May-Dracka, T. L. New Natural Products as New Leads for Antibacterial Drug Discovery. *Bioorg. Med. Chem. Lett.* **2014**, *24* (2), 413−418.

(6) Brown, D. G.; May-Dracka, T. L.; Gagnon, M. M.; Tommasi, R. Trends and Exceptions of Physical Properties on Antibacterial Activity for Gram-Positive and Gram-Negative Pathogens. *J. Med. Chem.* **2014**, *57* (23), 10144−10161.

(7) Lewis, K. Platforms for Antibiotic Discovery. *Nat. Rev. Drug Discovery* **2013**, *12* (5), 371−387.

(8) Brown, E. D.; Wright, G. D. Antibacterial Drug Discovery in the Resistance Era. *Nature* **2016**, *529* (7586), 336−343.

(9) Rothe, W. Das Neue Antibiotikum Xanthocillin. *Dtsch. Med. Wochenschr.* **1954**, *79*, 1080−1081.

(10) Emsermann, J.; Kauhl, U.; Opatz, T. Marine Isonitriles and Their Related Compounds. *Mar. Drugs* **2016**, *14* (1), 16.

(11) Edenborough, M. S.; Herbert, R. B. Naturally Occurring Isocyanides. *Nat. Prod. Rep.* **1988**, *5* (3), 229−245.

(12) Tsunakawa, M.; Kobaru, S.; Murata, S.; Oki, T.; Ohkusa, N.; Narita, Y.; Sawada, Y. Bu-4704, a New Member of the Xanthocillin Class. *J. Antibiot.* **1993**, *46* (4), 687−688.

(13) Isshiki, K.; Takahashi, Y.; Okada, M.; Sawa, T.; Hamada, M.; Naganawa, H.; Takita, T.; Takeuchi, T.; Umezawa, H.; Yamamoto, M.; Tatsuta, K. A New Antibiotic Indisocin and *N*-Methylindisocin. *J. Antibiot.* **1987**, *40* (8), 1195−1198.

(14) Chang, C. W. J.; Patra, A.; Roll, D. M.; Scheuer, P. J.; Matsumoto, G. K.; Clardy, J. Kalihinol-A, a Highly Functionalized Diisocyano Diterpenoid Antibiotic from a Sponge. *J. Am. Chem. Soc.* **1984**, *106* (16), 4644−4646.

(15) Di Blasio, B.; Fattorusso, E.; Magno, S.; Mayol, L.; Pedone, C.; Santacroce, C.; Sica, D. Axisonitrile-3, Axisothiocyanate-3 and Axamide-3. Sesquiterpenes with a Novel Spiro[4,5]Decane Skeleton from the Sponge *Axinella Cannabina*. *Tetrahedron* **1976**, *32* (4), 473−478.

(16) Miyaoka, H.; Shimomura, M.; Kimura, H.; Yamada, Y.; Kim, H.-S.; Yusuke, W. Antimalarial Activity of Kalihinol A and New Relative Diterpenoids from the Okinawan Sponge, Acanthella Sp. *Tetrahedron* **1998**, *54* (44), 13467−13474.

(17) Wang, L.; Zhu, M.; Zhang, Q.; Zhang, X.; Yang, P.; Liu, Z.; Deng, Y.; Zhu, Y.; Huang, X.; Han, L.; Li, S.; He, J. Diisonitrile Natural Product SF2768 Functions As a Chalkophore That Mediates Copper Acquisition in *Streptomyces thioluteus*. *ACS Chem. Biol.* **2017**, *12* (12), 3067−3075.

(18) Shang, Z.; Li, X.; Meng, L.; Li, C.; Gao, S.; Huang, C.; Wang, B. Chemical Profile of the Secondary Metabolites Produced by a Deep-Sea Sediment-Derived Fungus *Penicillium commune* SD-118. *Chin. J. Oceanol. Limnol.* **2012**, *30* (2), 305−314.

(19) Takatsuki, A.; Tamura, G.; Arima, K. New Antiviral Antibiotics; Xanthocillin X Mono- and Dimethylether, and Methoxy-Xanthocillin X Dimethylether. *J. Antibiot.* **1968**, *21* (12), 676−680.
(20) Tacconelli, E.; Carrara, E.; Savoldi, A.; Harbarth, S.; Mendelson, M.; Monnet, D. L.; Pulcini, C.; Kahlmeter, G.; Kluytmans, J.; Carmeli, Y.; Ouellette, M.; Outterson, K.; Patel, J.; Cavaleri, M.; Cox, E. M.; Houchens, C. R.; Grayson, M. L.; Hansen, P.; Singh, N.; Theuretzbacher, U.; Magrini, N.; Aboderin, A. O.; Al-Abri, S. S.; Awang Jalil, N.; Benzonana, N.; Bhattacharya, S.; Brink, A. J.; Burkert, F. R.; Cars, O.; Cornaglia, G.; Dyar, O. J.; Friedrich, A. W.; Gales, A. C.; Gandra, S.; Giske, C. G.; Goff, D. A.; Goossens, H.; Gottlieb, T.; Guzman Blanco, M.; Hryniewicz, W.; Kattula, D.; Jinks, T.; Kanj, S. S.; Kerr, L.; Kieny, M. P.; Kim, Y. S.; Kozlov, R. S.; Labarca, J.; Laxminarayan, R.; Leder, K.; Leibovici, L.; Levy-Hara, G.; Littman, J.; Malhotra-Kumar, S.; Manchanda, V.; Moja, L.; Ndoye, B.; Pan, A.; Paterson, D. L.; Paul, M.; Qiu, H.; Ramon-Pardo, P.; Rodríguez-Baño, J.; Sanguinetti, M.; Sengupta, S.; Sharland, M.; Si-Mehand, M.; Silver, L. L.; Song, W.; Steinbakk, M.; Thomsen, J.; Thwaites, G. E.; van der Meer, J. W.; Van Kinh, N.; Vega, S.; Villegas, M. V.; Wechsler-Fördös, A.; Wertheim, H. F. L.; Wesangula, E.; Woodford, N.; Yilmaz, F. O.; Zorzet, A. Discovery, Research, and Development of New Antibiotics: The WHO Priority List of Antibiotic-Resistant Bacteria and Tuberculosis. *Lancet Infect. Dis.* **2018**, *18* (3), 318−327.
(21) Galli, U.; Tron, G. C.; Purghè, B.; Grosa, G.; Aprile, S. Metabolic Fate of the Isocyanide Moiety: Are Isocyanides Pharmacophore Groups Neglected by Medicinal Chemists? *Chem. Res. Toxicol.* **2020**, *33* (4), 955−966.
(22) Wright, A. D.; Wang, H.; Gurrath, M.; König, G. M.; Kocak, G.; Neumann, G.; Loria, P.; Foley, M.; Tilley, L. Inhibition of Heme Detoxification Processes Underlies the Antimalarial Activity of Terpene Isonitrile Compounds from Marine Sponges. *J. Med. Chem.* **2001**, *44* (6), 873−885.
(23) Zhu, M.; Wang, L.; Zhang, W.; Liu, Z.; Ali, M.; Imtiaz, M.; He, J. Diisonitrile-Mediated Reactive Oxygen Species Accumulation Leads to Bacterial Growth Inhibition. *J. Nat. Prod.* **2020**, *83* (5), 1634−1640.
(24) Lakemeyer, M.; Zhao, W.; Mandl, F. A.; Hammann, P.; Sieber, S. A. Thinking Outside the Box−Novel Antibacterials to Tackle the Resistance Crisis. *Angew. Chem., Int. Ed.* **2018**, *57* (44), 14440−14475.
(25) Wright, M. H.; Sieber, S. A. Chemical Proteomics Approaches for Identifying the Cellular Targets of Natural Products. *Nat. Prod. Rep.* **2016**, *33* (5), 681−708.
(26) Lim, F. Y.; Won, T. H.; Raffa, N.; Baccile, J. A.; Wisecaver, J.; Rokas, A.; Schroeder, F. C.; Keller, N. P. Fungal Isocyanide Synthases and Xanthocillin Biosynthesis in. *mBio* **2018**, DOI: 10.1128/mBio.00785-18.
(27) Herbert, R. B.; Mann, J. The Incorporation of C_1 Units in the Biosynthesis of Tuberin and Xanthocillin. *J. Chem. Soc., Chem. Commun.* **1984**, *22*, 1474.
(28) Beiersdorf, R.; Ahrens, W. Untersuchungen Über die antibakteriellen und pharmakodynamischen Eigenschaften des neuen Antibioticums Xanthocillin. *Pharmazie* **1953**, *8* (10), 796−801.
(29) Yamaguchi, T.; Miyake, Y.; Miyamura, A.; Ishiwata, N.; Tatsuta, K. Structure-Activity Relationships of Xanthocillin Derivatives as Thrombopoietin Receptor Agonist. *J. Antibiot.* **2006**, *59* (11), 729−734.
(30) Shapiro, J. A.; Morrison, K. R.; Chodisetty, S. S.; Musaev, D. G.; Wuest, W. M. Biologically Inspired Total Synthesis of Ulbactin F, an Iron-Binding Natural Product. *Org. Lett.* **2018**, *20* (18), 5922−5926.
(31) Knight, D.; Dimitrova, D. D.; Rudin, S. D.; Bonomo, R. A.; Rather, P. N. Mutations Decreasing Intrinsic β-Lactam Resistance Are Linked to Cell Division in the Nosocomial Pathogen *Acinetobacter baumannii*. *Antimicrob. Agents Chemother.* **2016**, *60* (6), 3751−3758.
(32) Fonović, M.; Bogyo, M. Activity-Based Probes as a Tool for Functional Proteomic Analysis of Proteases. *Expert Rev. Proteomics* **2008**, *5* (5), 721−730.
(33) Evans, M. J.; Cravatt, B. F. Mechanism-Based Profiling of Enzyme Families. *Chem. Rev.* **2006**, *106* (8), 3279−3301.
(34) Cox, J.; Hein, M. Y.; Luber, C. A.; Paron, I.; Nagaraj, N.; Mann, M. Accurate Proteome-Wide Label-Free Quantification by Delayed Normalization and Maximal Peptide Ratio Extraction, Termed MaxLFQ. *Mol. Cell. Proteomics* **2014**, *13* (9), 2513−2526.
(35) Baba, T.; Ara, T.; Hasegawa, M.; Takai, Y.; Okumura, Y.; Baba, M.; Datsenko, K. A.; Tomita, M.; Wanner, B. L.; Mori, H. Construction of *Escherichia coli* K-12 in-Frame, Single-Gene Knockout Mutants: The Keio Collection. *Mol. Syst. Biol.* **2006**, DOI: 10.1038/msb4100050.
(36) Yamazaki, Y.; Niki, H.; Kato, J. Profiling of *Escherichia coli* Chromosome Database. In *Methods in Molecular Biology*; Humana Press, Inc.: Clifton, N.J., 2008; pp 385−389.
(37) Goodall, E. C. A.; Robinson, A.; Johnston, I. G.; Jabbari, S.; Turner, K. A.; Cunningham, A. F.; Lund, P. A.; Cole, J. A.; Henderson, I. R. The Essential Genome of *Escherichia coli* K-12. *mBio* **2018**, *9* (1), 1−18.
(38) Gallagher, L. A.; Ramage, E.; Weiss, E. J.; Radey, M.; Hayden, H. S.; Held, K. G.; Huse, H. K.; Zurawski, D. V.; Brittnacher, M. J.; Manoil, C. Resources for Genetic and Genomic Analysis of Emerging Pathogen *Acinetobacter baumannii*. *J. Bacteriol.* **2015**, *197* (12), 2027−2035.
(39) Frankenberg, N.; Moser, J.; Jahn, D. Bacterial Heme Biosynthesis and Its Biotechnological Application. *Appl. Microbiol. Biotechnol.* **2003**, *63* (2), 115−127.
(40) Lucidi, M.; Runci, F.; Rampioni, G.; Frangipani, E.; Leoni, L.; Visca, P. New Shuttle Vectors for Gene Cloning and Expression in Multidrug-Resistant *Acinetobacter* Species. *Antimicrob. Agents Chemother.* **2018**, *62* (4), 1−19.
(41) Frankenberg, N.; Erskine, P. T.; Cooper, J. B.; Shoolingin-Jordan, P. M.; Jahn, D.; Heinz, D. W. High Resolution Crystal Structure of a Mg^{2+}-Dependent Porphobilinogen Synthase. *J. Mol. Biol.* **1999**, *289* (3), 591−602.
(42) Heinemann, I. U.; Jahn, D.; Schulz, C.; Kobayashi, Y.; Jahn, M.; Awa, Y.; Heinz, D. W.; Wang, Y.-G.; Wachi, M.; Schubert, W.-D. Structure of the Heme Biosynthetic *Pseudomonas aeruginosa* Porphobilinogen Synthase in Complex with the Antibiotic Alaremycin. *Antimicrob. Agents Chemother.* **2010**, *54* (1), 267−272.
(43) Bollivar, D. W.; Clauson, C.; Lighthall, R.; Forbes, S.; Kokona, B.; Fairman, R.; Kundrat, L.; Jaffe, E. K. *Rhodobacter capsulatus* Porphobilinogen Synthase, a High Activity Metal Ion Independent Hexamer. *BMC Biochem.* **2004**, *5* (1), 17.
(44) Montagu, A.; Joly-Guillou, M.-L.; Rossines, E.; Cayon, J.; Kempf, M.; Saulnier, P. Stress Conditions Induced by Carvacrol and Cinnamaldehyde on *Acinetobacter baumannii*. *Front. Microbiol.* **2016**, *7* (JUL), 1−9.
(45) Tomaras, A. P.; Dorsey, C. W.; Edelmann, R. E.; Actis, L. A. Attachment to and Biofilm Formation on Abiotic Surfaces by *Acinetobacter baumannii*: Involvement of a Novel Chaperone-Usher Pili Assembly System. *Microbiology* **2003**, *149* (12), 3473−3484.
(46) Choi, A. H. K.; Slamti, L.; Avci, F. Y.; Pier, G. B.; Maira-Litrán, T. The PgaABCD Locus of *Acinetobacter baumannii* Encodes the Production of Poly-β-1−6-*N*-Acetylglucosamine, Which Is Critical for Biofilm Formation. *J. Bacteriol.* **2009**, *191* (19), 5953−5963.
(47) Xiao, Z.; Xu, P. Acetoin Metabolism in Bacteria. *Crit. Rev. Microbiol.* **2007**, *33* (2), 127−140.
(48) Yoon, E. J.; Chabane, Y. N.; Goussard, S.; Snesrud, E.; Courvalin, P.; Dé, E.; Grillot-Courvalin, C. Contribution of Resistance-Nodulation-Cell Division Efflux Systems to Antibiotic Resistance and Biofilm Formation in *Acinetobacter baumannii*. *mBio* **2015**, *6* (2), 1−13.
(49) Vestergaard, M.; Nøhr-Meldgaard, K.; Ingmer, H. Multiple Pathways towards Reduced Membrane Potential and Concomitant Reduction in Aminoglycoside Susceptibility in *Staphylococcus aureus*. *Int. J. Antimicrob. Agents* **2018**, *51* (1), 132−135.
(50) Dekic, S.; Hrenovic, J.; van Wilpe, E.; Venter, C.; Goic-Barisic, I. Survival of Emerging Pathogen *Acinetobacter baumannii* in Water

Environment Exposed to Different Oxygen Conditions. *Water Sci. Technol.* **2019**, *80* (8), 1581−1590.
(51) Deng, W. L.; Chang, H. Y.; Peng, H. L. Acetoin Catabolic System of *Klebsiella pneumoniae* CG43: Sequence, Expression, and Organization of the *aco* Operon. *J. Bacteriol.* **1994**, *176* (12), 3527−3535.
(52) Tolner, B.; Ubbink-Kok, T.; Poolman, B.; Konings, W. N. Characterization of the Proton/Glutamate Symport Protein of *Bacillus subtilis* and Its Functional Expression in Escherichia Coli. *J. Bacteriol.* **1995**, *177* (10), 2863−2869.
(53) Noinaj, N.; Guillier, M.; Barnard, T. J.; Buchanan, S. K. TonB-Dependent Transporters: Regulation, Structure, and Function. *Annu. Rev. Microbiol.* **2010**, *64* (1), 43−60.
(54) Atamna, H.; Ginsburg, H. Heme Degradation in the Presence of Glutathione. *J. Biol. Chem.* **1995**, *270* (42), 24876−24883.
(55) Ponka, P. Cell Biology of Heme. *Am. J. Med. Sci.* **1999**, *318* (4), 241−256.
(56) Atamna, H.; Brahmbhatt, M.; Atamna, W.; Shanower, G. A.; Dhahbi, J. M. ApoHRP-Based Assay to Measure Intracellular Regulatory Heme. *Metallomics* **2015**, *7* (2), 309−321.
(57) Dailey, H. A.; Dailey, T. A.; Gerdes, S.; Jahn, D.; Jahn, M.; O'Brian, M. R.; Warren, M. J. Prokaryotic Heme Biosynthesis: Multiple Pathways to a Common Essential Product. *Microbiol. Mol. Biol. Rev.* **2017**, *81* (1), 1−62.
(58) Huang, W.; Liu, Q.; Zhu, E. Y.; Shindi, A. A. F.; Li, Y. Q. Rapid Simultaneous Determination of Protoporphyrin IX, Uroporphyrin III and Coproporphyrin III in Human Whole Blood by Non-Linear Variable-Angle Synchronous Fluorescence Technique Coupled with Partial Least Squares. *Talanta* **2010**, *82* (4), 1516−1520.
(59) Shepherd, M.; Dailey, H. A. A Continuous Fluorimetric Assay for Protoporphyrinogen Oxidase by Monitoring Porphyrin Accumulation. *Anal. Biochem.* **2005**, *344* (1), 115−121.
(60) Mancini, S.; Imlay, J. Bacterial Porphyrin Extraction and Quantification by LC/MS/MS Analysis. *Bio-Protocol* **2015**, *5* (19), 1−4.
(61) Morales, E. H.; Pinto, C. A.; Luraschi, R.; Muñoz-Villagrán, C. M.; Cornejo, F. A.; Simpkins, S. W.; Nelson, J.; Arenas, F. A.; Piotrowski, J. S.; Myers, C. L.; Mori, H.; Vásquez, C. C. Accumulation of Heme Biosynthetic Intermediates Contributes to the Antibacterial Action of the Metalloid Tellurite. *Nat. Commun.* **2017**, DOI: 10.1038/ncomms15320.
(62) Dewachter, L.; Herpels, P.; Verstraeten, N.; Fauvart, M.; Michiels, J. Reactive Oxygen Species Do Not Contribute to ObgE*-Mediated Programmed Cell Death. *Sci. Rep.* **2016**, *6*, 1−8.
(63) Vestergaard, M.; Paulander, W.; Leng, B.; Nielsen, J. B.; Westh, H. T.; Ingmer, H. Novel Pathways for Ameliorating the Fitness Cost of Gentamicin Resistant Small Colony Variants. *Front. Microbiol.* **2016**, *7*, 1−12.
(64) Mike, L. A.; Dutter, B. F.; Stauff, D. L.; Moore, J. L.; Vitko, N. P.; Aranmolate, O.; Kehl-Fie, T. E.; Sullivan, S.; Reid, P. R.; DuBois, J. L.; Richardson, A. R.; Caprioli, R. M.; Sulikowski, G. A.; Skaar, E. P. Activation of Heme Biosynthesis by a Small Molecule That Is Toxic to Fermenting *Staphylococcus aureus*. *Proc. Natl. Acad. Sci. U. S. A.* **2013**, *110* (20), 8206−8211.
(65) Anderson, S. E.; Sherman, E. X.; Weiss, D. S.; Rather, P. N. Aminoglycoside Heteroresistance in *Acinetobacter baumannii* AB5075. *mSphere* **2018**, *3* (4), 1−12.
(66) Thöny-Meyer, L. Biogenesis of Respiratory Cytochromes in Bacteria. *Microbiol. Mol. Biol. Rev.* **1997**, *61* (3), 337−376.
(67) Ramsey, M.; Hartke, A.; Huycke, M. The Physiology and Metabolism of enterococci. In *Enterococci: From Commensals to Leading Causes of Drug Resistant Infection*; 2014; pp 1−55.
(68) Zapf, S.; Hoßfeld, M.; Anke, H.; Velten, R.; Steglich, W. Darlucins A and B, New Isocyanide Antibiotics from *Sphaerellopsis filum* (*Darluca filum*). *J. Antibiot.* **1995**, *48* (1), 36−41.
(69) Tyanova, S.; Temu, T.; Sinitcyn, P.; Carlson, A.; Hein, M. Y.; Geiger, T.; Mann, M.; Cox, J. The Perseus Computational Platform for Comprehensive Analysis of (Prote)Omics Data. *Nat. Methods* **2016**, *13* (9), 731−740.

https://dx.doi.org/10.1021/acscentsci.0c01621
ACS Cent. Sci. 2021, 7, 488−498